



Free water corrected diffusion tensor imaging discriminates between good and poor outcomes of comatose patients after cardiac arrest

Hanneke M. Keijzer^{1,2} · Marco Duering^{3,4} · Ofer Pasternak⁵ · Frederick J. A. Meijer⁶ · Marlous M. L. H. Verhulst^{1,7} · Bart A. R. Tonino⁸ · Michiel J. Blans⁹ · Cornelia W. E. Hoedemaekers¹⁰ · Catharina J. M. Klijn² · Jeannette Hofmeijer^{1,7}

Received: 25 May 2022 / Revised: 26 August 2022 / Accepted: 16 October 2022 / Published online: 24 November 2022
© The Author(s) 2022

Abstract

Objectives Approximately 50% of comatose patients after cardiac arrest never regain consciousness. Cerebral ischaemia may lead to cytotoxic and/or vasogenic oedema, which can be detected by diffusion tensor imaging (DTI). Here, we evaluate the potential value of free water corrected mean diffusivity (MD) and fractional anisotropy (FA) based on DTI, for the prediction of neurological recovery of comatose patients after cardiac arrest.

Methods A total of 50 patients after cardiac arrest were included in this prospective cohort study in two Dutch hospitals. DTI was obtained 2–4 days after cardiac arrest. Outcome was assessed at 6 months, dichotomised as poor (cerebral performance category 3–5; $n = 20$) or good ($n = 30$) neurological outcome. We calculated the whole brain mean MD and FA and compared between patients with good and poor outcomes. In addition, we compared a preliminary prediction model based on clinical parameters with or without the addition of MD and FA.

Results We found significant differences between patients with good and poor outcome of mean MD (good: $726 [702–740] \times 10^{-6} \text{ mm}^2/\text{s}$ vs. poor: $663 [575–736] \times 10^{-6} \text{ mm}^2/\text{s}$; $p = 0.01$) and mean FA (0.30 ± 0.03 vs. 0.28 ± 0.03 ; $p = 0.03$). An exploratory prediction model combining clinical parameters, MD and FA increased the sensitivity for reliable prediction of poor outcome from 60 to 85%, compared to the model containing clinical parameters only, but confidence intervals are overlapping.

Conclusions Free water-corrected MD and FA discriminate between patients with good and poor outcomes after cardiac arrest and hold the potential to add to multimodal outcome prediction.

Key Points

- Whole brain mean MD and FA differ between patients with good and poor outcome after cardiac arrest.
- Free water-corrected MD can better discriminate between patients with good and poor outcome than uncorrected MD.
- A combination of free water-corrected MD (sensitive to grey matter abnormalities) and FA (sensitive to white matter abnormalities) holds potential to add to the prediction of outcome.

Catharina J. M. Klijn and Jeannette Hofmeijer contributed equally to this work.

✉ Hanneke M. Keijzer
HMKeijzer@rijnstate.nl

¹ Department of Neurology, Rijnstate Hospital, P.O. box 9555, 6800 TA Arnhem, The Netherlands

² Department of Neurology, Donders Institute for Brain, Cognition, and Behaviour, Radboud University Medical Centre, 6500 HC Nijmegen, The Netherlands

³ Institute for Stroke and Dementia Research (ISD), University Hospital LMU, 81377 Munich, Munich, Germany

⁴ Medical Image Analysis Centre (MIAC AG), Basel and qbig, Department of Biomedical Engineering, University of Basel, CH-4051 Basel, Switzerland

⁵ Departments of Psychiatry and Radiology, Brigham and Women's Hospital, Harvard Medical School, Boston, MA 02115, USA

⁶ Department of Radiology and Nuclear Medicine, Radboud University Medical Centre, 6500 HC Nijmegen, The Netherlands

⁷ Department of Clinical Neurophysiology, Faculty of Science and Technology, University of Twente, 7522 NB Enschede, The Netherlands

⁸ Department of Radiology, Rijnstate Hospital, 6800 TA Arnhem, The Netherlands

⁹ Department of Intensive Care Medicine, 6800 TA, Rijnstate Hospital, Arnhem, The Netherlands

¹⁰ Department of Intensive Care Medicine, Radboud University Medical Centre, 6500 HC Nijmegen, The Netherlands

Keywords Brain edema · Brain ischaemia · Brain imaging · Cardiac arrest · MRI

Abbreviations

%MD ₄₅₀	Percentage of brain volume with MD < 450 × 10 ⁻⁶ mm ² /s
CPC	Cerebral performance category
CSF	Cerebrospinal fluid
DTI	Diffusion tensor imaging
DWI	Diffusion-weighted imaging
FA	Fractional anisotropy
FSL	fMRI brain Software Library
MD	Mean diffusivity
OHCA	Out of hospital cardiac arrest
SSEP	Somatosensory evoked potential
WLST	Withdrawal of life-sustaining treatment

Introduction

Postanoxic encephalopathy is the main cause of death in comatose patients after cardiac arrest and successful resuscitation. Approximately 50% of patients admitted to the intensive care unit (ICU) will never regain consciousness because of severe postanoxic encephalopathy [1, 2]. Early prediction of neurological outcome is important for multiple reasons. Accurate early prediction of poor outcome prevents patients from undergoing futile long-term and expensive treatment in an ICU, whereas premature treatment withdrawal is avoided for patients with relevant chances of recovery. Over the past years, substantial research efforts have resulted in prognostic electrophysiological [3, 4] and imaging parameters [5, 6]. However, current clinical prognostic measures yield only moderate predictive properties, with a reported accuracy of prediction of good or poor outcome in 30–70% of patients [3, 5–8].

The pathophysiological processes of postanoxic encephalopathy are important to understand when searching for possible predictors, but complex [9, 10]. Cerebral ischaemia starts with the failure of synaptic neurotransmission [11]. In case of severe or lasting ischaemia and ATP depletion, cell swelling or cytotoxic oedema occurs within minutes to days after cardiac arrest. Starting after one to two days, dysfunction of the blood-brain barrier may result in an inflow of plasma in the interstitial space, called vasogenic oedema [10].

Diffusion-weighted imaging (DWI) is sensitive to diffusion restriction within the brain [12]. Diffusion Tensor Imaging (DTI) is a model that combines several DWI measurements collected along different orientations. DTI can characterise both the magnitude and the direction of water diffusion, thus probing the brain tissue microstructure [13]. Two DTI measures are of particular interest: mean diffusivity (MD) reflects the magnitude of diffusion and fractional anisotropy (FA) its

directionality. Cytotoxic oedema leads to diffusion restriction, which is reflected by lower MD values, most prominent at 2–5 days after cardiac arrest [12, 14, 15]. Therefore, optimal discrimination by diffusion imaging is expected in this time window.

On the other hand, vasogenic oedema may increase MD due to the influx of water in the interstitial space [16]. Also, the dilution effects of vasogenic and cytotoxic oedema within the white matter results in a decrease in FA [17].

CSF has vastly different diffusion properties than brain tissue and is thus a prominent confounder of diffusion metrics in regions susceptible to partial volume effects. DTI analyses corrected for free water might provide a more specific measure of tissue damage by minimising the effect of CSF and vasogenic oedema [18, 19]. This is especially relevant in cortical areas, that are sensitive to hypoxia, but suffer greatly from CSF partial volume effects.

Previous studies have shown group differences and promising predictive values of diffusivity and FA between patients with good and poor outcomes. However, the overall quality of evidence is limited due to the often-retrospective study designs, variable timing of MRI, and a broad range of reported predictive values [5, 6, 8, 20–24].

Here, we study free water-corrected MD and FA in patients with good and poor outcomes after cardiac arrest and evaluate the potential to add to the multimodal prediction of neurological outcome. To estimate the additional value of MD and FA as predictors, we combine these with several parameters that are used in current clinical care in an exploratory prediction model for neurological outcome after cardiac arrest.

Materials and methods

We performed a prospective multicentre cohort study on the outcome prediction of comatose patients after cardiac arrest. Patients were included in two Dutch hospitals, Rijnstate hospital and Radboud University Medical Centre (Radboudumc). The study was approved by the Committee on Research Involving Human Subjects region Arnhem-Nijmegen and registered on clinicaltrials.gov (identifier: NCT03308305). For the current analyses, we used brain MRI data of day 3 ± 1 after cardiac arrest, collected between June 2018 and November 2020.

Patients

We included consecutive patients after permission from their legal representatives within 72 h after cardiac arrest. Inclusion criteria were as follows: cardiac arrest based on a cardiac

cause (including pulmonary embolism), Glasgow Coma Scale ≤ 8 at admission, age ≥ 18 years, and admission to the ICU. Exclusion criteria were: pregnancy, life expectancy < 24 h post cardiac arrest, any known progressive brain illness, pre-existing dependency in daily living, or a contraindication to undergo MRI scanning (e.g. presence of a pacemaker or foreign metal objects).

Patients were treated according to international guidelines [8, 25], as described in the local ICU protocols. Targeted temperature management at 36°C (Rijnstate Hospital) or $32\text{--}34^{\circ}\text{C}$ (Radboudumc) was induced after arrival at the ICU and maintained for 24 h. Upon rewarming, normothermia was actively maintained. Patients generally received (a combination of) propofol, midazolam, morphine, or sufentanil for sedation and analgesia.

Withdrawal of life-sustaining treatment (WLST) was considered at ≥ 72 h after cardiac arrest, during normothermia, and off sedation. Decisions on WLST were based on international guidelines including the absence of brainstem reflexes, treatment-resistant myoclonus, and bilateral absence of somatosensory evoked potentials (SSEPs) after reaching normothermia and depletion of sedative medicines [25]. Since April 2019, visual classification of the EEG is part of the Dutch guideline “prognosis of postanoxic coma.” Poor outcome is predicted with suppressed EEG at > 12 h after cardiac arrest or low voltage, burst suppression with identical bursts, or generalised periodic discharges on a suppressed background at > 24 h [26]. Decision-making regarding WLST always took into account the specific background of the patient and involved consultation of a multidisciplinary team and the patient’s family. In case of doubt, the decision was postponed and the patient was re-evaluated at a later time. MRI was never included in decisions on treatment withdrawal.

The primary outcome measure was “good” (CPC 1–2, no to mild neurological impairments) or “poor” (CPC 3–5, severe neurological impairments, vegetative state or death) neurological outcome at six months after cardiac arrest, as recommended by the International Liaison Committee on Resuscitation [27]. CPC scores were estimated by a standardised telephone interview based on the EuroQol-6D questionnaire, by an investigator (H.K., M.V.) blinded to the clinical course of the patient, EEG, and MRI readings.

Data acquisition

All patients underwent a 3-T MRI scan at 3 ± 1 days after cardiac arrest (Philips Ingenia (Rijnstate) or Siemens Skyra (Radboudumc), one scanner per site). For this study, we used 3D T1-weighted (Siemens: MPRAGE, voxel size $0.9 \times 0.9 \times 1.0$ mm, Philips: 3D TFE, voxel size $1.0 \times 1.0 \times 1.0$ mm), and 2D diffusion-weighted imaging sequences (Siemens: voxel size $2.0 \times 2.0 \times 2.0$ mm, 1 non-diffusion weighted image, 30 images with a b-value of 1000 s/mm^2 , TR/TE 9700/95 ms; Philips:

voxel size $2.0 \times 2.0 \times 2.0$ mm, 1 non-diffusion weighted image, 32 images with a b-value of 1000 s/mm^2 , TR/TE 9000/95 ms). Further details are listed in Supplementary Table 1.

Data analyses

Pre-processing of the DTI data consisted of the reduction of thermal noise and removal of Gibbs artefacts (MRtrix version 3.0 [28], dwidnoise and dwidgibbs), followed by correction for Eddy current distortions and motion (“EDDY”; fMRI brain Software Library (FSL); v6.0.2 [29]). Raw data and results of pre-processing were visually checked for quality and erroneous results and artefacts.

Diffusion measures were estimated both with and without free water correction. Diffusion models were calculated based on a nonlinear regularised minimisation process implemented in MATLAB (version R2016a, The MathWorks Inc.) [18]. For conventional DTI, a single tensor was directly fit on pre-processed data. For free water correction, a model with two tensors, representing two different diffusion compartments, was fit in each voxel. A fixed, isotropic tensor was used to model freely diffusing extracellular water (free water compartment). A second tensor was used to model the remaining signal, i.e. the signal originating from restricted water in tissue. Free water-corrected FA and MD were calculated from the tissue compartment’s tensor.

Individual FA maps were registered to a standard space (FMRIB58_FA) using the Tract-Based Spatial Statistics pipeline in FSL [30]. MD maps were co-registered to standard space using the subject-specific transformations obtained with FA maps. Voxel by voxel group comparisons of MD and FA between patients with good and poor outcome were performed using the FSL function “randomize” including the Threshold-Free Cluster Enhancement option [31]. This resulted in a family-wise error-corrected group difference map, where clusters with a p value < 0.01 were considered significantly different between patients with good and poor outcome. Patients with pre-existing structural abnormalities, such as atrophy, were excluded from the voxel-by-voxel comparisons, because of limited precision for registration to the standard space.

In all patients, we created whole brain masks from the T1 image using FSL’s Brain Extraction Tool (BET) and linearly registered those to the diffusion images in native space. We calculated mean MD and FA within these masks, using in-house created MATLAB scripts and FSLmaths. For the MD images uncorrected for free water, all voxels with $\text{ADC} < 200 \times 10^{-6}$ or $> 2000 \times 10^{-6} \text{ mm}^2/\text{s}$ were removed to exclude artefacts and influence of cerebral spinal fluid (CSF) [5, 15, 32]. In addition, we calculated the percentage of voxels with $\text{MD} < 450 \times 10^{-6} \text{ mm}^2/\text{s}$ within the whole brain mask ($\% \text{MD}_{450}$). This cut-off value was established after visual

inspection of the MD images and corresponds with previously proposed cut-off values of the ADC [33, 34].

EEGs were classified offline and blinded to the timing of the epoch, the patient's clinical status, MRI, and outcome. A computer randomly presented 5-minute artefact-free EEG epochs at 6, 12, 24, 36, 48, and 72 h after cardiac arrest to two reviewers (H.K., M.V.). EEG registrations were classified into three categories: (I) suppressed pattern with or without superimposed synchronous activity ≥ 24 h, (II) continuous activity ≤ 12 h, or (III) other patterns (Supplementary Table 2) [3, 35]. In case of disagreement, a consensus was determined by consultation with a third reviewer (J.H.).

Statistical analyses

Data are presented as mean and standard deviation (SD) when normally distributed, or median [interquartile range (IQR)], otherwise. For group comparisons, we used chi-squared, student *t*-tests, or Mann-Whitney *U* tests, where appropriate. *p* values < 0.05 were assumed statistically significant. Effect sizes were calculated using Cohen's *d*. Results of the voxel-by-voxel comparisons are presented as spatial maps of areas with statistically significant differences between patients with good and poor outcome at a *p* value < 0.01 .

To estimate the potential additional value of MD and FA for multimodal prediction of neurological outcome, we created four different logistic regression models using 10-fold cross-validation. The first model is the clinical model, consisting of three continuous (age, duration of the arrest, first measured lactate) and two categorical (sex, EEG classification) parameters, currently used in clinical assessment. The second model consisted of mean FA and MD after free water correction. The third model combined the clinical model with mean FA and mean MD. We then performed a sensitivity analysis with the fourth model, replacing mean MD with %MD₄₅₀.

Predictive values of the models were evaluated using receiver operating characteristics (ROC), area under the curve (AUC), maximal sensitivity to detect poor outcome without false positives, and sensitivity to predict good outcome with 90% specificity, in line with the recommendations in the European guideline [8].

Statistical analyses were performed using R version 3.5.3 and MATLAB.

Results

Of 261 screened comatose patients after cardiac arrest, 50 patients were included, and 20 (40%) had a poor outcome. The main reasons for exclusion were a non-cardiac cause ($n = 44$), and no permission from the legal representative ($n = 48$; Supplementary Figure 1).

Patient characteristics are listed in Table 1. Four subjects (two with poor outcome) were excluded from the voxel-based comparisons, because of structural deficits hampering registration to the standard space. These included large ventricles in three elderly patients and one patient with a recent stroke.

Mean diffusivity

Patients with poor outcome had lower MD in large parts of the cortical grey and white matter than patients with good outcome in voxel-based comparisons (Fig. 1A). These differences were most prominent in the occipital and parietal regions. The deep grey nuclei and deep white matter showed no differences in MD between patients with good and poor outcome. In patients with poor outcome, the median MD of the whole brain was lower than in patients with good outcome, with a large effect size (Table 2). MD values of Siemens and Philips MRI were comparable (Fig. 2A).

Repeating analyses with MD uncorrected for free water yielded smaller brain areas with group differences in the voxel-wise analysis, and smaller effect sizes in the whole brain analysis (Cohen's *d* 1.06 and 0.84 with and without free water correction respectively, Table 2; Supplementary Table 3). Therefore, only free water corrected measures were included in all the following analyses.

The %MD₄₅₀ was higher in patients with poor neurological outcome than in those with good outcome (18% vs. 3%, Table 2). In 55% of the patients with poor outcome, $> 11\%$ of the brain showed an MD $< 450 \times 10^{-6}$ mm²/s, versus 0% in the patients with good outcome.

Fractional anisotropy

Patients with poor outcome had widespread lower FA values in the cerebral white matter than patients with good outcome in voxel-based comparisons (Fig. 1B). We found no differences in FA values in the cortex and deep grey nuclei.

Furthermore, the mean FA of the whole brain was lower in patients with poor outcome than in patients with good outcome, with a medium effect size (Table 2). FA values of Siemens and Philips MRI were comparable (Fig. 2B).

Potential predictive value

The clinical model was able to predict good outcome with 93% (78–100 95% CI) sensitivity at 90% specificity and poor outcome with 60% (37–80%) sensitivity at 100% specificity. Prediction model two, consisting of DTI measures alone (mean MD and FA) predicted good outcome with 43% (25–60%) sensitivity and poor outcome with 60% (33–81%) sensitivity (Fig. 3). Prediction model three, combining the clinical model with mean MD and FA predicted good outcome with 93% (73–100%) and poor outcome with 85% (64–96%)

Table 1 Baseline characteristics

Characteristic	Good outcome (n = 30)	Poor outcome (n = 20)	p value
Age	56 ± 11	67 ± 11	< 0.01
Male	25 (83%)	14 (70%)	0.26
OHCA	30 (100%)	20 (100%)	NA
Shockable first rhythm	30 (100%)	15 (75%)	< 0.01
Duration of resuscitation (min)	12 [10–15]	23 [19–31]	< 0.01
First lactate measured	3.6 [2.7–6.7]	4.1 [3.1–5.4]	0.57
GCS Motor score ≤ 3 at day 3	1 (3%)	15 (75%)	< 0.01
Bilaterally absent pupillary light response ≥ 72 h	0 (0%)	4 (20%)	0.01
SSEP performed	0 (0%)	16 (80%)	< 0.01
Absent SSEP response	0 (0%)	4 (25%)	0.01
EEG: continuous ≤ 12 h	15 (50%)	1 (5%)	< 0.01
EEG: suppressed pattern with or without superimposed synchronous activity ≥ 24 h	0 (0%)	3 (15%)	0.03
Time to MRI (h)	76 ± 24	77 ± 25	0.94
CPC score:			
- 1	13 (43)	0	
- 2	17 (57)	0	
- 3	0	3 (15)	
- 4	0	0 (0)	
- 5	0	17 (85)	

Outcome is based on 6-month follow-up. Data are presented as n (%) for dichotomous variables, mean ± sd for normally distributed continuous variables, and median [IQR] otherwise. *CPC*, cerebral performance category; *OHCA*, out-of-hospital cardiac arrest

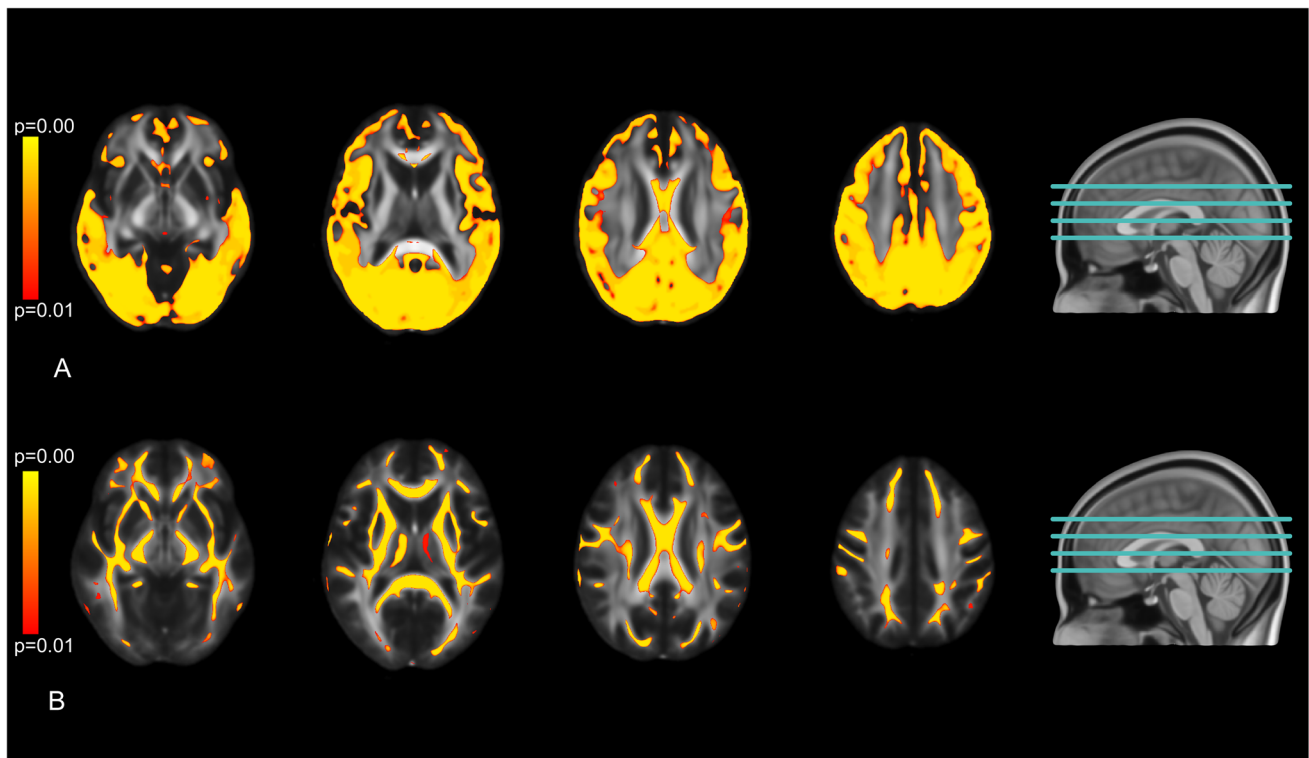


Fig. 1 A spatial distribution of differences in mean diffusivity and **(B)** fractional anisotropy after free water correction. Coloured areas show brain areas where patients with poor neurological outcome show significantly lower values than patients with good neurological outcome ($p < 0.01$)

Table 2 Whole-brain mean diffusivity, fractional anisotropy, and percentage of brain volume with mean diffusivity below the threshold of $450 \times 10^{-6} \text{ mm}^2/\text{s}$

Parameter	Good outcome	Poor outcome	<i>p</i> value	Effect size
Mean diffusivity*	726 [702–740]	663 [575–736]	0.01	1.06 (0.44–1.67)
Fractional anisotropy	0.30 ± 0.03	0.28 ± 0.03	0.03	0.65 (0.06–1.24)
%MD ₄₅₀ (%)	3.4 [1.8–6.4]	18.0 [5.8–32.8]	< 0.01	1.31 (0.67–1.95)

Data are represented as *n* (%) for dichotomous variables, mean \pm sd for normally distributed continuous variables and median [IQR] otherwise. Effect size is depicted as Cohen's *d* (95% CI). MD, mean diffusivity; %MD₄₅₀, brain volume with mean diffusivity below the threshold of $450 \times 10^{-6} \text{ mm}^2/\text{s}$; *MD $\times 10^{-6} \text{ mm}^2/\text{s}$

sensitivity. The sensitivity analysis with model four, combining the clinical model with mean FA and %MD₄₅₀ yielded similar results as model three, with prediction of good outcome with 97% (85–100%) sensitivity and poor outcome with 80% (57–95%) sensitivity (Fig. 3). Summarising, the addition of DTI parameters to the clinical model does not increase the sensitivity for prediction of good outcome. Sensitivity for the prediction of poor outcome without false positives increased. However, confidence intervals are overlapping.

Discussion

Patients with poor neurological outcome after cardiac arrest show lower free water corrected MD, FA, and higher %MD₄₅₀ than patients with good outcome. Exploratory prediction models suggest that these MRI parameters hold potential to add to multimodal outcome prediction of comatose patients after cardiac arrest.

Our results are aligned with previous studies, that have shown group differences and relevant predictive values of diffusivity measures. These studies showed utility for the apparent diffusion coefficient (ADC) derived from conventional DWI sequences [5, 6, 20, 36], and for radial and axial diffusivity based on the DTI sequence [23, 37]. The MD measure derived in our study is equivalent to ADC, but while ADC is

estimated from three diffusion directions, MD is more robustly estimated from 30 and 32 diffusion directions in our study. Aligned with the previous studies, we report a decrease in diffusivity in patients with poor outcome, most prevalent in the cortical grey matter. This can be explained by the high sensitivity to hypoxia of the GM. A post mortem study of patients who died two to five days after cardiac arrest (a timing similar to our MRI measurements) also showed a high prevalence of grey matter injury [38].

The additional predictive value of diffusion imaging appears to be high for the prediction of a poor neurological outcome and limited for the prediction of good outcome. Reliable prediction of poor outcome is important in clinical care, because it helps in determining if prolonged intensive life-supporting treatment is justified for a specific patient. When poor outcome cannot be predicted, treatment will generally be continued. Although (absence of) prediction of a good outcome will usually have a limited effect on the continuation of care, it supports communication between doctors and patients' relatives and may aid in the decisions on the escalation of organ support [39].

Unlike previous studies, the MD measure in our study is free water corrected. Reported predictive values of ADC and MD vary greatly between studies. CSF contamination of the cortical grey matter is a possible cause for these discrepancies. CSF contamination and other free water influx are influenced

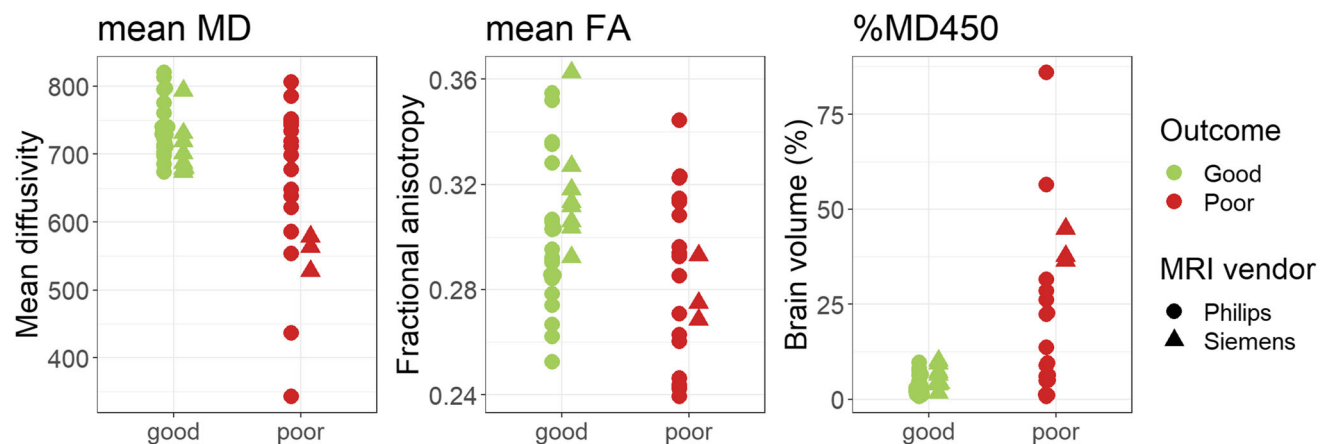


Fig. 2 Whole-brain mean diffusivity (MD), fractional anisotropy (FA), and percentage of brain volume with MD $< 450 \times 10^{-6} \text{ mm}^2/\text{s}$ after free water correction for individual patients with good and poor outcome, differentiated by scanner site

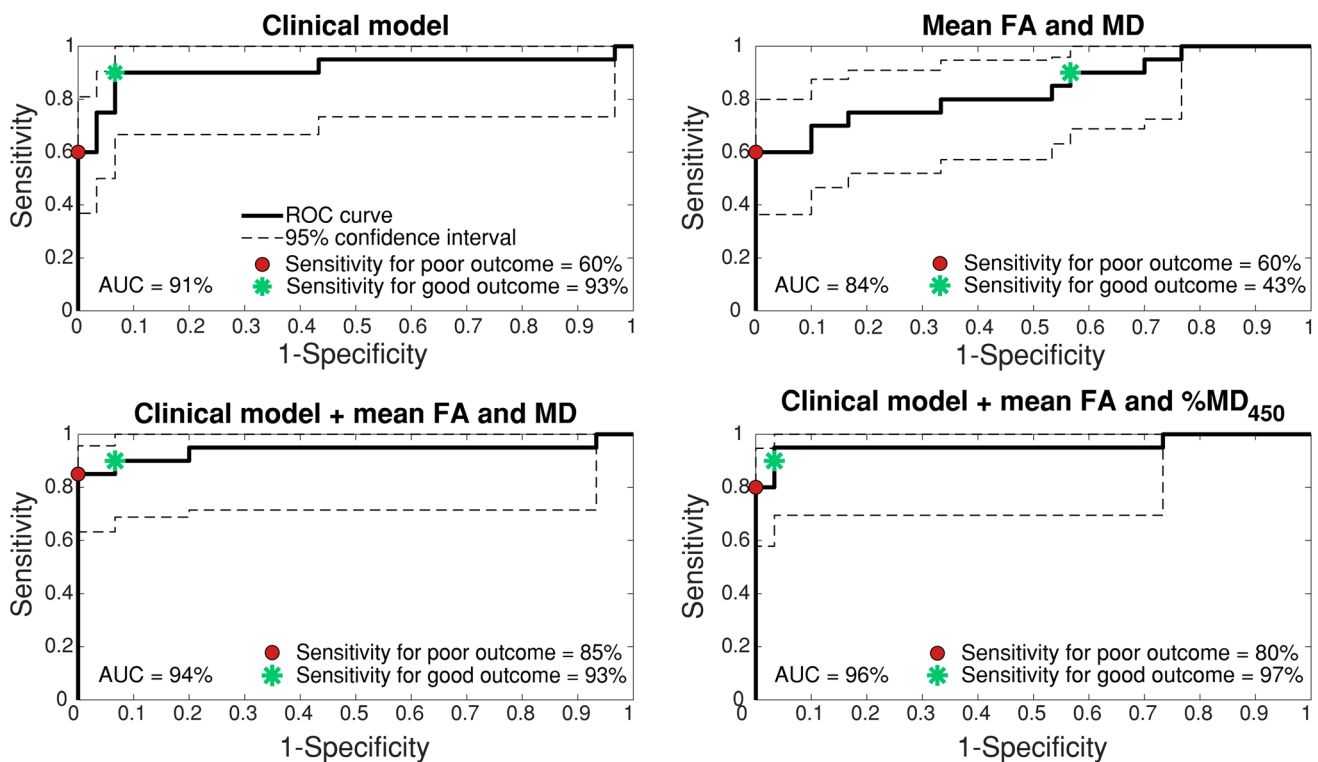


Fig. 3 Receiver Operated Characteristic curves with 95% confidence interval of 4 logistic regression models with 10-fold cross-validation. The clinical models are based on age, sex, duration of resuscitation, shockable first rhythm, first measured lactate, and EEG classification.

Specificity level for poor outcome is set at 100%, for good outcome at 90%. %MD₄₅₀, percentage of brain volume with MD < 450 × 10⁻⁶ mm²/s; AUC, area under the curve

by subject positioning, ventricle and subarachnoid space volume, hydration level, inflammation, and body temperature [40]. These factors can vary greatly across and within patients in the first days after cardiac arrest. This variation is reduced by using free water elimination techniques [40]. We found that free water-corrected MD yielded a higher effect size for discrimination between good and poor outcomes than uncorrected MD and allowed the identification of group differences in more areas of the brain.

While we found MD differences in the cortical grey matter, we did not find MD differences in the subcortical grey matter when comparing between patients with good and poor outcome. Differences in subcortical grey matter were observed in previous DWI studies [5, 6, 20], and were explained by the high metabolic demand of the deep grey nuclei [41]. However, a previous study on global ischaemia in a dog model found higher sensitivity to ischaemia in the cortex than in the basal ganglia [42]. This, together with the early and strict timing of our MRI scans possibly explains the lack of differences in the subcortical grey matter.

Differences in FA were most prominent in the white matter, with lower values in poor than in good outcome patients. Lower FA values in the white matter indicate less prominent directionality of diffusion along the white matter tract. Within the white matter, oligodendrocytes are responsible for

myelinisation and are highly sensitive to hypoxia and hypoglycaemia [9, 43]. Swelling of the oligodendrocytes is an early response to ischaemia, followed by necrosis in more severe hypoxia [44]. This is followed by demyelination and swelling of the axons [44]. Both processes could explain the reduced FA in the white matter. The FA measure is less effective in identifying differences in the grey matter, since FA in healthy grey matter is already low. The effects of FA in the white matter complement those of MD in the grey matter, and both measures are thus useful to consider together in analyses.

Adding MD and FA measures to a prediction model based on parameters used in current clinical care improved predictive values in our cohort. Our predictive values are in line with predictive values previously reported by studies using ADC, MD, and FA [5, 6, 20, 22, 24, 36]. However, since the clinical parameters of the models have been used in decisions regarding WLST, we can only estimate the potential additional value of DTI to current clinical parameters. Absolute predictive values are prone to the self-fulfilling prophecy. In clinical practice, MRI will probably be performed when combined clinical and electrophysiological measurements and biomarkers preclude definite prediction of outcome.

Strengths of this study are the prospective study design, the early and strict timing of MRI and EEG measurements, and the multimodal approach. This study also has limitations.

First, the sample size is relatively small, leading to a possible overestimation of our results, especially with regard to prediction. We also had to exclude four patients for the voxel-based analyses, due to pre-existent structural brain deficits, such as atrophy. Second, as in all studies on outcome prediction after cardiac arrest, we cannot fully exclude the influence of the self-fulfilling prophecy, since the withdrawal of life-sustaining treatment always results in poor outcome. However, MRI measures were not taken into account in decisions on treatment withdrawal. Third, the use of different MRI scanners could potentially affect our results, but this influence seemed to be small. Future studies could also improve the diffusion MRI acquisition to include multi-slice and multi-shell techniques which will make the acquisition faster and the model fit more robust, respectively.

Multiple steps are necessary before DTI imaging can be used as a prognosticator in daily clinical practice. First, the results of this study should be validated in a large, independent sample. Since each MRI scanner introduces a possible bias, vendor-specific cut-off values may improve results, but are difficult to validate. To prevent further bias, it is important to harmonise scan protocols and the processing of the data after acquisition [45]. Including the acquisition of a phase-encode reversed $b = 0$ image within the scan protocol could further improve data preprocessing, including a correction for field inhomogeneities and susceptibility artefacts. Validated and automated pipelines could then help clinicians to perform these analyses in a standardised fashion.

In conclusion, a combination of free water-corrected MD (sensitive to grey matter abnormalities) and FA (sensitive to white matter abnormalities) holds the potential to add to the prediction of good and poor outcome of comatose patients after cardiac arrest.

Supplementary Information The online version contains supplementary material available at <https://doi.org/10.1007/s00330-022-09245-w>.

Acknowledgements The authors thank Ruud van Kaam, a technical physician at the ICU of the Radboudumc, Yvonne Teitink and Helene Vogelensang, research nurses at the Rijnstate hospital, the staff of the ICU, radiology, and clinical neurophysiology departments, and technical medicine students for constructive assistance in obtaining informed consent and performing EEG measurements and MRI scans.

Funding HMK is funded by the Rijnstate-Radboud promotion fund. OP is funded by two grants from the National Institute of Health (NIH) (grant numbers: NIH P41EB015902 and NIH R01MH074794). CJMK is supported by a clinically established investigator grant from the Dutch Heart Foundation (Grant Number 2012T077) and an ASPASIA grant from The Netherlands Organisation for Health Research and Development, ZonMw (grant number 015008048). JH is supported by a clinically established investigator grant from the Dutch Heart Foundation (Grant Number 2018T070)

Declarations

Guarantor The scientific guarantor of this publication is Prof. Dr. J. Hofmeijer.

Conflict of interest The authors of this manuscript declare no relationships with any companies whose products or services may be related to the subject matter of the article.

Statistics and biometry No complex statistical methods were necessary for this paper.

Informed consent Written informed consent was obtained from all subjects (patients) and/or their legal representatives in this study.

Ethical approval Institutional Review Board approval was obtained.

Methodology

- prospective
- diagnostic or prognostic
- multicentre study

Open Access This article is licensed under a Creative Commons Attribution 4.0 International License, which permits use, sharing, adaptation, distribution and reproduction in any medium or format, as long as you give appropriate credit to the original author(s) and the source, provide a link to the Creative Commons licence, and indicate if changes were made. The images or other third party material in this article are included in the article's Creative Commons licence, unless indicated otherwise in a credit line to the material. If material is not included in the article's Creative Commons licence and your intended use is not permitted by statutory regulation or exceeds the permitted use, you will need to obtain permission directly from the copyright holder. To view a copy of this licence, visit <http://creativecommons.org/licenses/by/4.0/>.

References

1. Laver S, Farrow C, Turner D, Nolan J (2004) Mode of death after admission to an intensive care unit following cardiac arrest. *Intensive Care Med* 30:2126–2128
2. Lemiale V, Dumas F, Mongardon N et al (2013) Intensive care unit mortality after cardiac arrest: the relative contribution of shock and brain injury in a large cohort. *Intensive Care Med* 39:1972–1980
3. Ruijter BJ, Tjepkema-Cloostermans MC, Tromp SC et al (2019) Early electroencephalography for outcome prediction of postanoxic coma: a prospective cohort study. *Ann Neurol* 86:203–214
4. Bongiovanni F, Romagnosi F, Barbella G et al (2020) Standardized EEG analysis to reduce the uncertainty of outcome prognostication after cardiac arrest. *Intensive Care Med* 46:963–972
5. Hirsch KG, Fischbein N, Mlynash M et al (2020) Prognostic value of diffusion-weighted MRI for post-cardiac arrest coma. *Neurology* 94:e1684–e1692

6. Keijzer HM, Hoedemaekers CWE, Meijer FJA, Tonino BAR, Klijn CJM, Hofmeijer J (2018) Brain imaging in comatose survivors of cardiac arrest: pathophysiological correlates and prognostic properties. *Resuscitation* 133:124–136
7. Sandroni C, D'Arrigo S, Cacciola S et al (2020) Prediction of poor neurological outcome in comatose survivors of cardiac arrest: a systematic review. *Intensive Care Med* 46:1803–1851
8. Nolan JP, Sandroni C, Bottiger BW et al (2021) European Resuscitation Council and European Society of Intensive Care Medicine guidelines 2021: post-resuscitation care. *Intensive Care Med*. <https://doi.org/10.1007/s00134-021-06368-4>
9. Busl KM, Greer DM (2010) Hypoxic-ischemic brain injury: pathophysiology, neuropathology and mechanisms. *NeuroRehabilitation* 26:5–13
10. Sekhon MS, Ainslie PN, Griesdale DE (2017) Clinical pathophysiology of hypoxic ischemic brain injury after cardiac arrest: a "two-hit" model. *Crit Care* 21:90
11. Hofmeijer J, van Putten MJ (2012) Ischemic cerebral damage: an appraisal of synaptic failure. *Stroke* 43:607–615
12. von Kummer R, Dzialowski I (2017) Imaging of cerebral ischemic edema and neuronal death. *Neuroradiology* 59:545–553
13. Soares JM, Marques P, Alves V, Sousa N (2013) A hitchhiker's guide to diffusion tensor imaging. *Front Neurosci* 7:31
14. Mlynash M, Campbell DM, Leproust EM et al (2010) Temporal and spatial profile of brain diffusion-weighted MRI after cardiac arrest. *Stroke* 41:1665–1672
15. Bevers MB, Scirica BM, Avery KR, Henderson GV, Lin AP, Lee JW (2018) Combination of clinical exam, MRI and EEG to predict outcome following cardiac arrest and targeted temperature management. *Neurocrit Care* 29:396–403
16. Parekh MB, Gurjarpadhye AA, Manoukian MA, Dubnika A, Rajadas J, Inayathullah M (2015) Recent developments in diffusion tensor imaging of brain. *Radiol Open J* 1:1
17. Rai V, Nath K, Saraswat VA, Purwar A, Rathore RK, Gupta RK (2008) Measurement of cytotoxic and interstitial components of cerebral edema in acute hepatic failure by diffusion tensor imaging. *J Magn Reson Imaging* 28:334–341
18. Pasternak O, Sochen N, Gur Y, Intrator N, Assaf Y (2009) Free water elimination and mapping from diffusion MRI. *Magn Reson Med* 62:717–730
19. Metzler-Baddeley C, O'Sullivan MJ, Bells S, Pasternak O, Jones DK (2012) How and how not to correct for CSF-contamination in diffusion MRI. *Neuroimage* 59:1394–1403
20. Vanden Berghe S, Cappelle S, De Keyser F et al (2020) Qualitative and quantitative analysis of diffusion-weighted brain MR imaging in comatose survivors after cardiac arrest. *Neuroradiology* 62:1361–1369
21. Barth R, Zubler F, Weck A et al (2020) Topography of MR lesions correlates with standardized EEG pattern in early comatose survivors after cardiac arrest. *Resuscitation* 149:217–224
22. Luyt C, Galanaud D, Perlberg V et al (2012) Diffusion tensor imaging to predict long-term outcome after cardiac arrest - a bicentric pilot study. *Anesthesiology* 117(6):1311–21. <https://doi.org/10.1097/ALN.0b013e318275148c>
23. van der Eerden AW, Khalilzadeh O, Perlberg V et al (2014) White matter changes in comatose survivors of anoxic ischemic encephalopathy and traumatic brain injury: comparative diffusion-tensor imaging study. *Neuroradiology* 270(2):506–16. <https://doi.org/10.1148/radiol.13122720>
24. Velly L, Perlberg V, Boulrier T et al (2018) Use of brain diffusion tensor imaging for the prediction of long-term neurological outcomes in patients after cardiac arrest: a multicentre, international, prospective, observational, cohort study. *Lancet Neurol* 17:317–326
25. Nolan JP, Soar J, Cariou A et al (2015) European Resuscitation Council and European Society of Intensive Care Medicine Guidelines for Post-resuscitation Care 2015: Section 5 of the European Resuscitation Council Guidelines for Resuscitation 2015. *Resuscitation* 95:202–222
26. (2019) Neurofysiologisch onderzoek postanoxisch coma. Federatie Medisch Specialisten. Available via https://richtlijnendatabase.nl/richtlijn/prognose_van_postanoxisch_coma/neurofysiologisch_onderzoek_postanoxisch_coma.html. Accessed 22-4-2021 2019
27. Perkins GD, Jacobs IG, Nadkarni VM et al (2015) Cardiac arrest and cardiopulmonary resuscitation outcome reports: update of the Utstein Resuscitation Registry Templates for Out-of-Hospital Cardiac Arrest: a statement for healthcare professionals from a task force of the International Liaison Committee on Resuscitation (American Heart Association, European Resuscitation Council, Australian and New Zealand Council on Resuscitation, Heart and Stroke Foundation of Canada, InterAmerican Heart Foundation, Resuscitation Council of Southern Africa, Resuscitation Council of Asia); and the American Heart Association Emergency Cardiovascular Care Committee and the Council on Cardiopulmonary, Critical Care, Perioperative and Resuscitation. *Circulation* 132:1286–1300
28. Tournier J-D, Smith R, Raffelt D et al (2019) MRtrix3: a fast, flexible and open software framework for medical image processing and visualisation. *Neuroimage* 202:116137
29. Andersson JLR, Sotiropoulos SN (2016) An integrated approach to correction for off-resonance effects and subject movement in diffusion MR imaging. *Neuroimage* 125:1063–1078
30. Smith SM, Jenkinson M, Johansen-Berg H et al (2006) Tract-based spatial statistics: voxelwise analysis of multi-subject diffusion data. *Neuroimage* 31:1487–1505
31. Winkler AM, Ridgway GR, Webster MA, Smith SM, Nichols TE (2014) Permutation inference for the general linear model. *Neuroimage* 92:381–397
32. Hirsch KG, Mlynash M, Eyngorn I et al (2016) Multi-center study of diffusion-weighted imaging in coma after cardiac arrest. *Neurocrit Care* 24:82–89
33. Reynolds AS, Guo X, Matthews E et al (2017) Post-anoxic quantitative MRI changes may predict emergence from coma and functional outcomes at discharge. *Resuscitation* 117:87–90
34. Moon HK, Jang J, Park KN et al (2018) Quantitative analysis of relative volume of low apparent diffusion coefficient value can predict neurologic outcome after cardiac arrest. *Resuscitation* 126:36–42
35. Tjepkema-Cloostermans MC, van Meulen FB, Meinsma G, van Putten MJAM (2013) A Cerebral Recovery Index (CRI) for early prognosis in patients after cardiac arrest. *Crit Care* 17:R252
36. Wouters A, Scheldeman L, Plessers S et al (2021) Added value of quantitative apparent diffusion coefficient values for neuroprognostication after cardiac arrest. *Neurology* 96:e2611–e2618
37. Laitio R, Hynninen M, Arola O et al (2016) Effect of inhaled xenon on cerebral white matter damage in comatose survivors of out-of-hospital cardiac arrest: a randomized clinical trial. *JAMA* 315:1120–1128
38. van Putten M, Jansen C, Tjepkema-Cloostermans MC et al (2019) Postmortem histopathology of electroencephalography and evoked potentials in postanoxic coma. *Resuscitation* 134:26–32
39. Sandroni C, D'Arrigo S, Cacciola S et al (2022) Prediction of good neurological outcome in comatose survivors of cardiac arrest: a systematic review. *Intensive Care Med* 48:389–413

40. Albi A, Pasternak O, Minati L et al (2017) Free water elimination improves test-retest reproducibility of diffusion tensor imaging indices in the brain: a longitudinal multisite study of healthy elderly subjects. *Hum Brain Mapp* 38:12–26
41. Tambasco N, Romoli M, Calabresi P (2018) Selective basal ganglia vulnerability to energy deprivation: Experimental and clinical evidences. *Prog Neurobiol* 169:55–75
42. Sieber FE, Palmon SC, Traystman RJ, Martin LJ (1995) Global incomplete cerebral ischaemia produces predominantly cortical neuronal injury. *Stroke* 26:2091–2095 discussion 2096
43. Lyons SA, Kettenmann H (1998) Oligodendrocytes and microglia are selectively vulnerable to combined hypoxia and hypoglycemia injury in vitro. *J Cereb Blood Flow Metab* 18:521–530
44. Pantoni L, Garcia JH, Gutierrez JA (1996) Cerebral white matter is highly vulnerable to ischaemia. *Stroke* 27:1641–1646 discussion 1647
45. Vollmar C, O'Muircheartaigh J, Barker GJ et al (2010) Identical, but not the same: intra-site and inter-site reproducibility of fractional anisotropy measures on two 3.0T scanners. *Neuroimage* 51: 1384–1394

Publisher's note Springer Nature remains neutral with regard to jurisdictional claims in published maps and institutional affiliations.